Available online at www.eccomasproceedia.org
Eccomas Proceedia COMPDYN (2023) 457-467

ECCOMAS
Proceedia

COMPDYN 2023
9th ECCOMAS Thematic Conference on
Computational Methods in Structural Dynamics and Earthquake Engineering
M. Papadrakakis, M. Fragiadakis (eds.)
Athens, Greece, 12-14 June 2023

STRUCTURAL HEALTH MONITORING OF THE FATIGUE BEHAVIOR OF FRP STRENGTHENED RC BEAMS

Barbara Charalambidi[1], Konstantinos Providakis[1], Konstantinos Katakalos[2] and Alexandros Charalampidis[2]

[1] Technical University of Crete, University Campus, Akrotiri 73100, Chania, Greece
e-mail: {vcharalampidi,kprovidakis}@tuc.gr

[2] Aristotle University of Thessaloniki, University Campus 54124, Thessaloniki, Greece
{kkatakal,alexchar}@civil.auth.gr

Abstract

Reinforced concrete structures exposed to fatigue loading are subjected to serious structural damage and high cost in repair and maintenance. Fatigue damage in critical RC members adversely impacts the ability of structures to withstand future operating conditions and increases the risk of fatal failures and catastrophic collapses if not controlled. Structural health monitoring (SHM) of such structural members through the measuring of deflections and steel strain may provide a safe approach towards an efficient assessment of end of life prior to the fragile fracture of steel. In this research program, 10 reinforced concrete beams are subjected to fatigue and monotonic loading. A real-time structural health monitoring system is applied on the RC beam specimens. The test set-up involves an array of smart piezoelectric transducers and strain gauges mounted on the steel and the FRP reinforcements of the specimens. Damage detection and evaluation is achieved using the in-situ measurements of the integrated sensor signals at the healthy state of the member and at various levels of damage during testing. The use of the smart PZT sensors aims to contribute to the development of a prevention model for the fatigue failure of FRP-strengthened beams. SHM of such beams through the measuring of deflections and steel strains may provide a safe approach towards an efficient assessment of end of life prior to the fragile fracture of steel. Moreover, SHM of the FRP retrofit may provide a margin to reassess and avoid fragile fracture of steel.

Keywords: Fatigue, FRP, Structural Health Monitoring, Reinforced Concrete, Piezoelectric sensors.

ISSN:2623-3347
Peer-review under responsibility of the organizing committee of COMPDYN 2023.
doi: 10.7712/120123.10413.20380

1 INTRODUCTION

The fatigue behavior of reinforced concrete beams and bridge girders has been a field of increased interest [1-11]. Several studies have identified experimentally and analytically the different parameters affecting the fatigue life of reinforced concrete beams, strengthened in bending through fiber reinforced polymers. In particular, the effect of the maximum stress and the stress range of the steel reinforcement to the fatigue behavior of the reinforced concrete beams has been investigated by several authors. The higher the maximum stress and the stress range on the longitudinal steel bars of the beam, the lower their fatigue life. ACI Committee 440.2R-08 guide [12] recommends stress limits for FRP strengthening under tension and concrete under compression as well as a peak reinforcing bar stress of 80% of yield strength to estimate the upper limit of fatigue loading in Serviceability Limit State. It is acknowledged by the existing literature that the critical material vulnerable to fatigue failure is steel and that stresses on steel about 60% of its yielding strength practically do not lead to fatigue failure [2, 5, 7, 11]. The available fatigue prediction models provide the number of cycles to failure with respect to the steel stress range [1,13] assuming indirectly a sustained load between a minimum and maximum level. The significant role of the ratio of the axial rigidity of the tensile steel bar ks to the axial rigidity of fiber reinforced polymer (FRP) strengthening kf plays in extending the fatigue life of steel and thus of RC FRP strengthened beams was indicated in [14]. The lower the ks/kf ratio, the higher the fatigue life of the retrofitted member.

Structural health monitoring (SHM) of such structural members through the measuring of deflections and steel strains may provide a safe approach towards an efficient assessment of end of life prior to the fragile fracture of steel. Once the failure mechanism is controlled and the steel fracture is prevented, the earlier the FRP strengthening and the lower the ks=kf (AsEs/AfEf) ratio of a retrofit, the longer the extension of the member's life [11]. Structural health monitoring even of the FRP retrofit may provide a margin to reassess and avoid fragile fracture of steel.

Piezoelectric smart materials application as a damage detection technique is a promising development in the field of structural health monitoring of reinforced concrete members and structures, showing increased reliability and robustness. It combines the advantages of PZTs such as its small size, lightweight, low cost, active-sensing capability, long-term stability and easy to apply character, increased sensitivity and efficiency in capturing localized damages in real-time utilizing high-frequency excitations without requirements of experienced technicians or complicated instrumentation [15-17]. First applications of PZT transducers for evaluation of the integrity of RC members showed promising results over other traditional non-destructive methods. The damage detection and localization ability of smart piezoceramic patches for real-life RC structures by monitoring a 5 m span RC bridge during its destructive load testing was examined in [18]. In-situ non-destructive evaluation for SHM of RC beams strengthened with carbon fiber reinforced polymer composite overlay using embedded piezoelectric wafer active sensors was performed in [19]. On-line monitoring of concrete compressive strength gain using smart PZT patches has successfully been achieved [20-23]. Numerical studies utilizing PZT sensors to detect and localize cracking in concrete beams and debonding damages in RC beams retrofitted with CFRP laminates have also been presented [24-26]. The detection of the flexural damages in the steel bars of the lower part of the mid-span area of a simply supported RC beam using PZT sensors was examined in [27].

In this research program, the application of a real-time structural health monitoring system is applied on the RC beam specimens subjected to cyclic loading. Damage detection and evaluation is achieved using the in-situ measurements of the deflections, steel strain measurements and the piezoelectric sensor signals during testing.

For the purposes of this research, 9 reinforced concrete beams were cast with web dimensions of 100 mm x 150 mm and 800 mm in length. Beams were strengthened in flexure and shear with externally bonded FRP reinforcement (Figure 1).

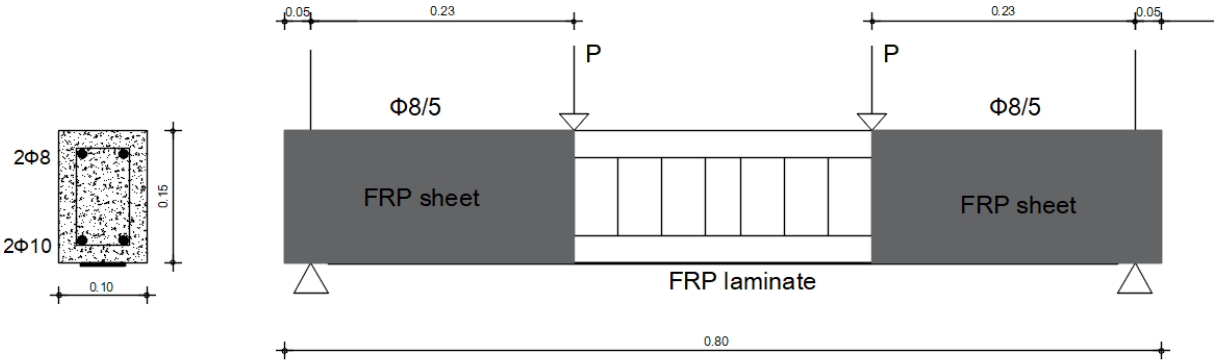

Figure 1: Concrete beam geometry, detailing of reinforcements, and FRP geometry

2 EXPERIMENTAL PROGRAM

2.1 Specimen geometry

Experiments conducted for this program involved nine reinforced concrete beams, measuring 100 mm wide x 150 mm deep x 800 mm long. Normal strength, ready-mixed concrete was used of 20 MPa nominal strength. The typical geometry of beams, reinforcement details and strengthening schemes are shown in Figure 1. The mechanical properties of the FRP sheets and laminates are cited in Table 1.

	FRP laminates	FRP sheets
E_f (N/mm^2)	165000	231000
ε_{fu}	0.018	0.017
f_{fu} (N/mm^2)	2900	4100
t_f (mm)	1.2	0.12

Table 1. Fiber reinforced polymers' properties

All beams had the same reinforcement configuration. The internal reinforcement consisted of two bottom bars of 10 mm diameter (As1= 157 mm2) and two top bars of 8 mm diameter (As2 = 100.48mm2). Stirrups of 8 mm diameter were placed in the beam as shear reinforcement, at a spacing of 50 mm. (Figure 1). Both longitudinal rebars and shear stirrups had a nominal yield stress of 500 MPa. Specimens were strengthened for both shear and flexure. Shear strengthening was accomplished with fully wrapped CFRP sheets with unidirectional fibers, at the shear spans of the beams. Sheets had a reported tensile strength of 4100 MPa, modulus of elasticity of 231 GPa and 0.12 mm thickness (system SikaWrap®-600C, product of Sika Hellas S.A.). To achieve flexural strengthening, the specimens were externally bonded with one carbon fiber laminate (CFRP laminates Sika® CarboDur® S512, product of Sika Hellas S.A.), with 2900 MPa strength, 165 GPa modulus of elasticity, 50 mm width and 1.2 mm thickness. The FRP strengthened beams were designed according to ACI Committee 440.2R-08.

2.2 Test Setup, Mode of Loading, and Instrumentation

Beams were tested under four point bending, at an average loading frequency of 1.3 Hz, using a 500 kN capacity MTS-810 servo-hydraulic dynamic actuator. The actuator was operated under load control for the fatigue loading. Table 2, provides a summary of the beams and of their loading pattern. Three different loading amplitudes were performed with different upper load limit, ranged from 20% of the design ultimate strength of the beam to the 80%, 90% and 100% of the strength corresponding to the nominal yield stress of the longitudinal reinforcement. A peak reinforcing bar stress of 80% of yield represents the upper limit recommended by ACI Committee 440 (2008). All beams were subjected to fatigue loading up to failure

Group	Spec.	Preloading before strengthening	Pmax(kN)	Pmin(kN)	Cycles	δPmax(mm)	δult(mm)
A	A1	Py	100%Py (103kN)	20%Py (20.5kN)	700	12.88	27.39
	A2	None	80%Py (85kN)		31670	4.05	18.08
	A3		90%Py (93kN)		47400	12.12	21.68
B	B1		90%Py (93kN)		9930	13.69	19.92
	B2		100%Py (103kN)		2040	12.84	21.24
	B3		80%Py (85kN)		234150	10.02	14.77
C	C1	Fatigue 20%-60%Py (up to 100.000 cycles)	90%Py (93kN)		47150	15.72	24.32
	C2		100%Py (103kN)		4455	11.32	20.75
	C3		80%Py (85kN)		61850	8.55	21.75

Table 2: Test results, load ranges, fatigue lives

Deflections at the midspan were recorded during testing, as well as strains on longitudinal steel and on CFRP laminates, and pzt measurements in order to study their variation under fatigue loading conditions. For that reason, an electrical resistance strain gauge and a piezoelectric sensor were attached at the midspan of the tensile longitudinal steel reinforcement, and an electrical resistance strain gauge was applied at the midspan of the CFRP laminate. The deflection at midspan was measured using two LVDTs placed at the 1/3 of beam's soffit. The experimental setup is illustrated in Figure 2.

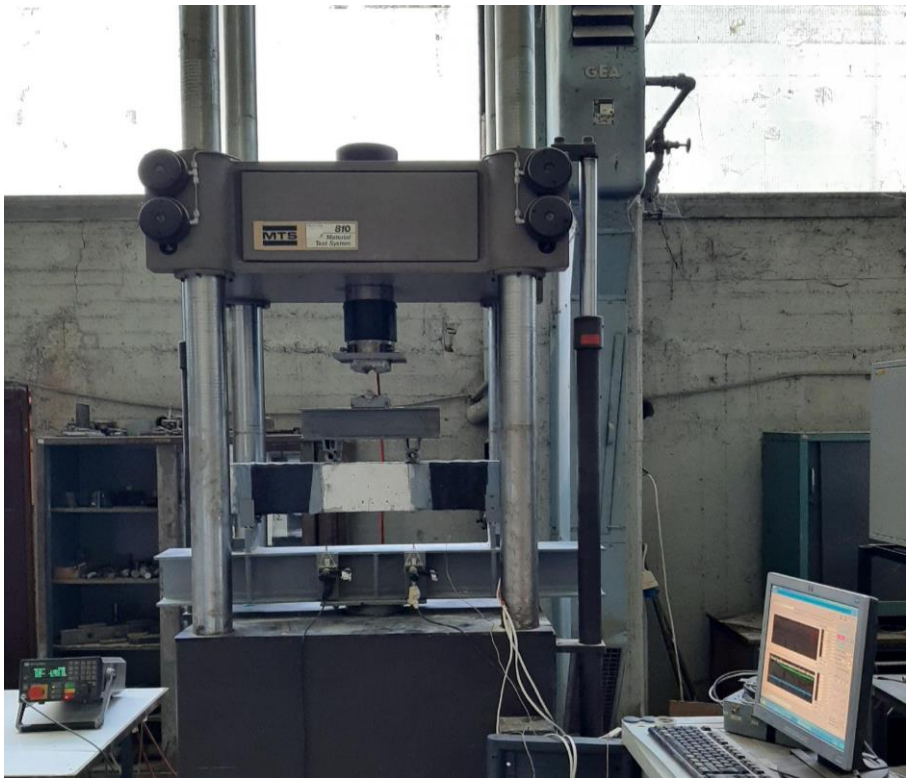

Figure 2: Experimental testing setup - Laboratory of Experimental Strength of Materials and Structures, Aristotle University of Thessaloniki

3 RESULTS AND DISCUSSION

3.1 Fatigue Tests

Nine beams were tested under fatigue loading in order to record their load-deflection and strain responses. Three different preloading patterns before strengthening were followed. Group A: Specimens A1, A2, A3 were subjected to monotonic loading until steel yielding. Then, the specimens were strengthened in bending and shear and subjected to fatigue loading until failure. Group B: No preloading was applied before strengthening and fatigue loading. Group C: Specimens C1, C2, C3 were subjected to fatigue loading for 100,000 cycles. Then, the specimens were strengthened in bending and shear and subjected to fatigue loading until failure. The minimum applied fatigue load for each beam of every group was equal to the 20% of their yielding load. The maximum applied load was equal to the 80%, the 90% and the 100% of the yielding load. Table 2 cites the preloading pattern, the maximum and minimum applied loads per cycle, the percentage of the maximum applied load to the design yielding load, and the percentage of the maximum applied load to the design yield load. It also cites the number of performed cycles and corresponding deflection during the fatigue tests.

3.2 Fatigue Life and Failure Mode

All beams failed due to fatigue loading. Failure was due to tensile fracture of the steel reinforcement. No prior fatigue failure of the concrete cover in between the steel bar and the FRP strengthening was recorded in any case. The concrete cover of the beams varied from 10 mm to 15 mm. No prior FRP debonding failure was recorded. In each specimen, one main crack was formed at the midspan region of the beam, between the two vertical loads. As the number of fatigue loading cycles was increased, an increase in the total number of cracks and in their

width was observed. During the last cycles, one particular crack was much wider than the rest of the recorded cracks. This main crack indicates the region where the steel fracture occurs [11]. Figures 3 and 4, illustrate the main crack in the case of beams B2 (beam with no preloading and 20%-80%Py fatigue load range) and A1(beam with static preloading up to Py and 20%-100% Py fatigue load range). The fractured bar after fatigue failure of beam A1 is illustrated in Figure 5. The fracture of the steel bar was sudden, with no evident necking around the fractured region. Debonding of the externally bonded FRP laminate was a secondary failure mechanism of the strengthened beams. Debonding of the laminate occurred after the fatigue failure of the steel reinforcement of the beams and expanded towards almost the whole midspan of the beam.

Figure 3: Crack pattern during testing of Beam B2 (no preloading, 20%-80%Py fatigue loading)

Figure 4: Crack pattern at failure of Beam A1 (Py preloading, 20%-100%Py fatigue loading)

Figure 5: Steel fracture after fatigue testing of Beam B2 (Py preloading, 20%-100%Py fatigue loading)

3.3 Deflection Curves

The mechanical behavior of the specimens is assessed through their deflection vs cycles diagrams. Figure 8 illustrates the variation of deflections with time for specimens A3, B2, C3. A stable region where the deflection remains relatively constant for many cycles is recorded. Then, an abrupt increase of deflection occurs just before failure (point A, Figure 6). This behavior was typical for all beams of the experimental program. Specimen A3, which was tested under 20% to 90% of Py, lasted 47,400 cycles, developed deflection from 12.12 mm (point A) to 21.68 mm at failure. Specimen B2, which was tested under 20% to 100% of Py, lasted 2,040 cycles, developed deflection from 12.84 mm (point A) to 21.24 mm at failure. Finally, specimen C3, which was tested under 20% to 80% of Py, lasted 61,850 cycles, developed deflection from 8.55 mm (point A) to 21.75 mm at failure.
The variable behavior of beams under high amplitude fatigue loading may be attributed to the different upper loading level.

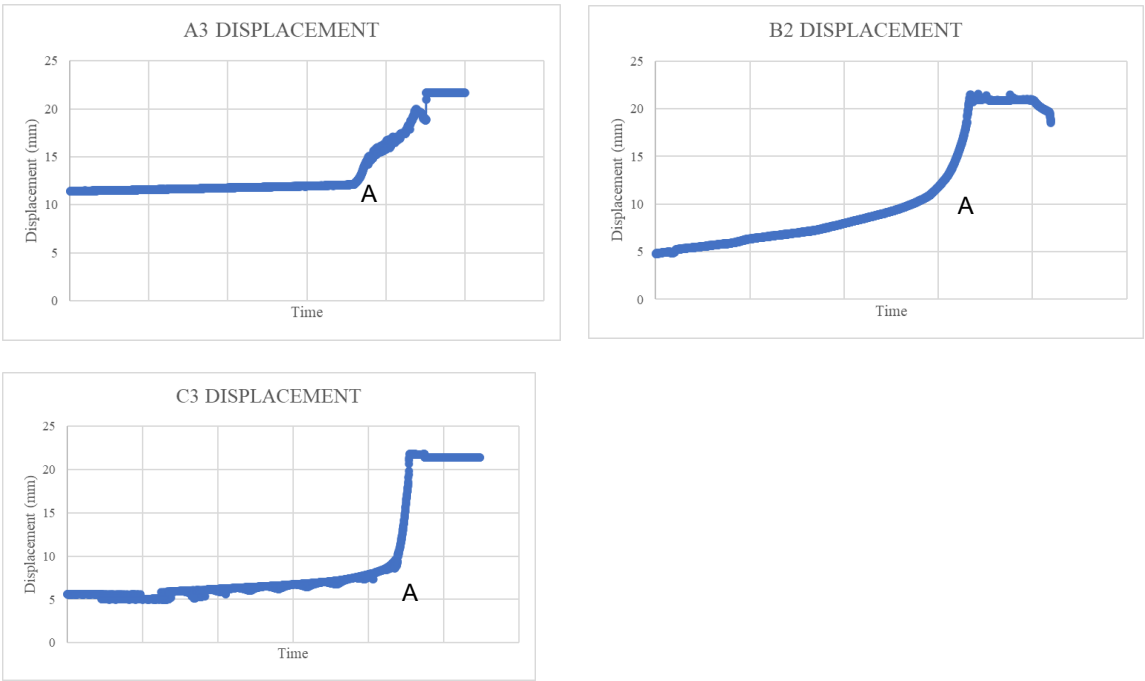

Figure 6: Deflection versus time curve for Specimens A3, B2, C3 (~90%Py, ~100%Py, ~80%Py respectively) during the last cycles of fatigue testing

The only mechanism to restrict the axial strain evolution due to fatigue in the steel reinforcement, is the elastic axial stiffness of the FRP that remains constant throughout loading (no debonding has been reported).

3.4 Tensile Behavior of Steel Bars and FRP Laminates and Piezoelectric sensor recordings

Strain variation of the middle steel bar of beam B1 (Figure 7) reveals a rather stable maximum strain around 1.5%, up to the last cycles of loading. Before failure, the strain on the steel abruptly increases. A strain gauge was placed at the midspan of FRP laminate in the specimen. A rather stable maximum strain around 2.6% was recorded up to the last cycles of loading, similar to the recordings that concern the steel reinforcement. Then, a sudden increase in strain occurs up to 4% strain (Figure 8). After that cycle, the specimen failed due to fatigue. The specimen failed with steel fracture due to fatigue loading. The FRP laminate could sustain the shock by the sudden fracture of the steel and maintain the residual bearing capacity. The comparative study of the two diagrams suggests that FRP strengthening can restrict the enormous extension of the steel bars close to fatigue failure. It can restrict the maximum tensile strain of steel and stabilize the overall response.

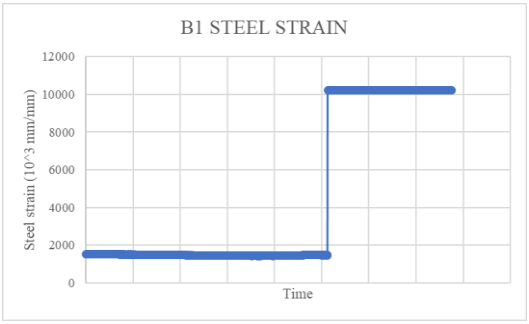

Figure 7: Steel strain versus time curve for Specimen B1 (~90%Py) during the last cycles of fatigue

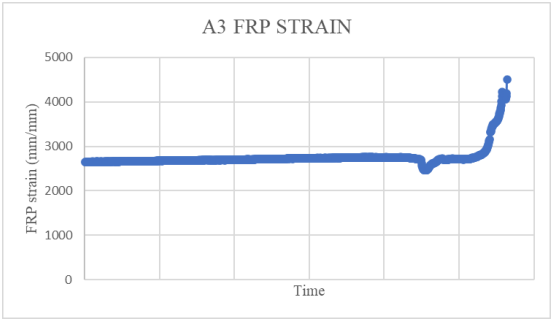

Figure 8: FRP strain versus time curve for Specimens A3(~90%Py) during the last cycles of fatigue

A response assessment of Beam C3 is illustrated in Figure 9 where the variation of PZT measurements is recorded. The PZT sensor was bonded in the midspan of the tensile steel bar. The response of the PZT is rather similar to the steel gauge and FRP gauge measurements. A stable maximum measurement of around 0.39V was recorded up to the last cycles of loading. Then, a sudden increase in measurements occurs up to 0.90V, following fatigue loading.

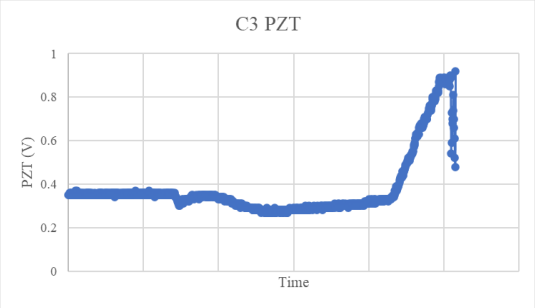

Figure 9: PZT recordings versus time curve for Specimens C3 (~80%Py) during the last cycles of fatigue

4 CONCLUSIONS

Nine reinforced concrete beams of rectangular cross section (100 x 150 mm) and 800 mm length were strengthened in bending and in shear with FRP techniques. Beams were separated in three groups A, B, C according to their loading scenario before strengthening. In Group A, the unstrengthened beams were subjected to monotonic loading up to yielding, in Group B there was no preloading before strengthening, and in Group C, the unstrengthened beams were subjected to fatigue loading of 100,000 cycle with a range of 20% - 60% of their yielding strength. Then, all specimens were strengthened and subjected to fatigue loading up to failure. In all cases of fatigue loading, the failure was due to tensile fracture of the steel reinforcement. The steel fracture was followed by FRP laminate debonding. Yielding of the reinforcing steel was not evident in the strain measurements of all beams, at the strain gauge's position, up to the last cycles of testing; then the steel exhibited a fragile fracture. Strain measurements on FRP reveal an interaction and partial restriction of unstable tensile strain evolution on the steel bar. One piezoelectric sensor was bonded at the midspan of a tensile steel bar. Damage assessment has been successfully attempted using piezoelectric sensors. The PZT recordings may contribute to the assessment of the fatigue life of beams.

The midspan deflections versus number of cycles curves suggest that in all cases, there was a stable midspan deflection proportional to the increase in cycles, remaining relatively constant. Then, an abrupt increase of deflection occurred just before failure. This overall behavior is in accordance with the abovementioned strain and PZT measurements.

The collective evidence from the present and previous studies reveals an adequate margin of cycles with significantly degraded behavior of the beams before failure. Structural health monitoring of such beams through the measuring of deflections and steel strains may provide a safe approach towards an efficient assessment of end of life prior to the fragile fracture of steel. Structural health monitoring via piezoelectric sensors may provide a margin to reassess and avoid the fragile fracture of steel.

5 ACKNOWLEDGMENT

This research is co-financed by Greece and the European Union (European Social Fund-ESF) through the Operational Programme «Human Resources Development, Education and Lifelong Learning» in the context of the project "Reinforcement of Postdoctoral Researchers - 2nd Cycle" (MIS-5033021), implemented by the State Scholarships Foundation (IKY).

The authors wish to thank Sika Hellas S.A. for providing the FRP materials and resins, TUC's Applied Mechanics Laboratory staff for the assistance in the construction, casting, and

preparation of the specimens, and AUTh's Experimental Strength of Materials and Structures Laboratory staff for the assistance in the FRP implementations and experimental testing.

REFERENCES

[1]P.S. Senthilnath, A. Belarbi, J.J. Myers, Performance of CFRP strengthened reinforced concrete beams in the presence of delaminations and lap slices under fatigue loading, *Proc., Int. Conf. on Composites in Construction (CCC-2001)*, Porto, Portugal, 323–328, 2001.

[2]C.G. Papakonstantinou, M.F. Petrou, K.A. Harries, Fatigue behavior of RC beams strengthened with GFRP sheets, *Journal of Composites for Construction*, **5**, 246–253, 2001.

[3]L. Bizindavyi, K.W. Neale, M.A. Erki, Experimental investigation of bonded fiber reinforced polymer-concrete joints under cyclic loading, *Journal of Composites for Construction*, **7**, 127–134, 2003.

[4]P.J. Heffernan, M.A. Erki, Fatigue Behavior of Reinforced Concrete Beams Strengthened with Carbon Fiber reinforced plastic laminates. *Journal of Composites for Construction*, **8**, 132-140, 2004.

[5]R. Gussenhoven, S. Brena, Fatigue behavior of reinforced concrete beams strengthened with different FRP laminate configurations, *Proc., 7th Fiber Reinforced Polymers for Reinforced Concrete Structures (FRPRCS7)*, American Concrete Institute (ACI), Farmington Hills, MI, 613–630, 2005.

[6]M. Ekenel, A. Rizzo, J.J. Myers, A. Nanni, Flexural fatigue behavior of reinforced concrete beams strengthened with FRP fabric and procured laminate systems, *Journal of Composites for Construction*, **10**, 433–442, 2006.

[7]C. Gheorgiu, P. Labossiere, J. Proulx, Response of CFRP strengthened beams under fatigue with different load amplitudes, *Construction and Building Materials*, **21**, 756–763, 2007.

[8]G. Williams, C. Higgins, Fatigue of diagonally cracked RC girders repaired with CFRP, *Journal of Bridge Engineering*, **13**, 24–33, 2008.

[9]K. Katakalos, C. Papakonstantinou, Fatigue of Reinforced Concrete Beams Strengthened with Steel-Reinforced Inorganic Polymers, *Journal of Composites for Construction*, **13**, 103-112, 2009.

[10]E. Ferrier, D. Bigaud, J.C. Clément, P. Hamelin, Fatigue loading effect on RC beams strengthened with externally bonded FRP, *Construction and Building Materials*, **25**, 539–546, 2011.

[11]B. Charalambidi, T. Rousakis, A. Karabinis, Fatigue behavior of large scale reinforced concrete beams strengthened in flexure with fiber reinforced polymer laminates, *Journal of Composites for Construction*, **20**, 2016.

[12]ACI Committee 440.2R-08, *Guide for the Design and Construction of Externally Bonded FRP Systems for Strengthening Concrete Structures*, American Concrete Institute, Michigan, 2008.

[13]H.M. Diab, Z. Wu, Review of existing fatigue results of beams externally strengthened with FRP laminates, *Fourth international conference on FRP composites in civil engineering (CICE2008)*, 22-24 July, Zurich, Switzerland, 2008.

[14]B. Charalambidi, T. Rousakis, A. Karabinis, Analysis of the fatigue behavior of reinforced concrete beams strengthened in flexure with fiber reinforced polymer laminates, Composites Part B, **96**, 69-78, 2016.

[15]V.G.M. Annamdas, C.K. Soh, Application of electromechanical impedance technique for engineering structures: review and future issues, *Journal of Intelligent Material Systems and Structures,***21**, 41–59, 2010.

[16]H.K. Jung, H. Jo, G. Park, D.L. Mascarenas, C.R. Farrar, Relative baseline features for impedance-based structural health monitoring, *Journal of Intelligent Material Systems and Structures,* **5**, 2294–2304, 2014.

[17]C.G. Karayannis, M.E. Voutetaki, C.E. Chalioris, C.P. Providakis, G.M. Angeli, Detection of flexural damage stages for RC beams using piezoelectric sensors (PZT), *Smart Structures and Systems*, **15**, 2015.

[18]C.K. Soh, K.K.-H. Tseng, S. Bhalla, A. Gupta, Performance of smart piezoceramic patches in health monitoring of a RC bridge, *Smart Structures and Systems,* **9** 533–542, 2000.

[19]V. Giurgiutiu, K. Harries, M. Petrou, J. Bost, J.B. Quattlebaum, Disbond detection with piezoelectric wafer active sensors in RC structures strengthened with FRP composite overlays, Earthquake Engineering and Engineering Vibration, **2**, 213–223, 2003.

[20]S.W. Shin, T.K. Oh, Application of electro-mechanical impedance sensing technique for online monitoring of strength development in concrete using smart PZT patches, *Construction and Building Materials*, **23**,1185–1188, 2009.

[21]D. Wang, H. Zhu, Monitoring of the strength gain of concrete using embedded PZT impedance transducer, *Construction and Building Materials*,**25**, 3703–3708, 2011.

[22]C.P. Providakis, E.V. Liarakos, T-WiEYE: an early-age concrete strength development monitoring and miniaturized wireless impedance sensing system, *Engineering Proceedings*, **10**, 484–489, 2011.

[23]C.P. Providakis, K.D. Stefanaki, M.E. Voutetaki, J. Tsompanakis, M.E. Stavroulaki , J. Agadakos, An integrated approach for structural health monitoring of concrete structures based on electromechanical admittance and guided waves. *Proceedings of 6th ECCOMAS Conference on Smart Structures and Materials*, Politecnico di Torino, 2013.

[24]M.E. Voutetaki, C.P. Providakis, C.E. Chalioris, FRP debonding prevention of strengthened concrete members under dynamic load using smart piezoelectric materials (PZT), *Proceedings of the 15th European Conference on Composite Materials*, ECCM 2012 – Composites at Venice, Venice; Italy, pp. 24–28, 2012.

[25]C.P. Providakis, T.C. Triantafillou, D. Karabalis, A. Papanicolaou, K. Stefanaki, A. Tsantilis, E. Tzoura, Simulation of PZT monitoring of reinforced concrete beams retrofitted with CFRP, *Smart Structures and Systems*, **14**, 811–830, 2014.

[26]C.P. Providakis, K.D. Stefanaki, M.E. Voutetaki, J. Tsompanakis, M.E. Stavroulaki, Damage detection in concrete structures using a simultaneously activated multi-mode PZT active sensing system: numerical modeling, *Structure and Infrastructure Engineering*, **10**, 1451–1468, 2014.

[27]C.G. Karayannis, M.E. Voutetaki, C.E. Chalioris, C.P. Providakis, G.M. Angeli, Detection of flexural damage stages for RC beams using piezoelectric sensors (PZT), *Smart Structures and Systems*, **15**, 997-1018, 2015.